Photophysical properties of stilbenes with imide groups

Veronika Strehmel [a,b,*], Curtis W. Frank [b], Bernd Strehmel [c]

[a] Institute of Technical and Macromolecular Chemistry, Martin-Luther-University, Halle-Wittenberg, Geusaer Straße, D-06217 Merseburg, Germany
[b] Department of Chemical Engineering, Stanford University, Stanford, CA 94305-5025, USA
[c] Institute of Physical and Theoretical Chemistry, Humboldt University of Berlin, Bunsenstraße 1, D-10117 Berlin, Germany

Abstract

Imide model compounds synthesized from 2,5-dimethoxy-4'-aminostilbene and different anhydrides, such as hexafluoroisopropylidene-2,2'-bis(phthalic anhydride), pyromellitic anhydride, 3,3',4,4'-benzophenone tetracarboxylic dianhydride and phthalic anhydride, were photochemically characterized by UV absorption spectroscopy and stationary and time-resolved fluorescence spectroscopy. The fluorescence measurements in solution showed the dominance of non-radiative processes at room temperature. The fluorescence decay curves were multiexponential, their course depending on the temperature and viscosity of the surroundings. Steady state fluorescence experiments were performed in various polymer matrices. The spectra obtained showed differences in the number of bands. The molecular structure and the alignment of the polymer influenced the emission behaviour of the imide model compounds. Furthermore, semiempirical quantum mechanical calculations indicated the dominance of a charge transfer for the HOMO–LUMO configuration from the stilbene skeleton to the imide subunit. Irradiation experiments in solution indicated the high photostability of all the compounds investigated. © 1997 Elsevier Science S.A.

Keywords: Charge transfer; Fluorescence spectroscopy; Polymer matrix; Quantum mechanical calculations; Stilbene

1. Introduction

Aromatic polyimides possess high thermal, thermo-oxidative and chemical stability coupled with a low dielectric constant and excellent mechanical properties. Polyimides are attractive materials for many applications, e.g. films, coatings, mouldings, semiconductors, adhesives and advanced composites, because of the favourable combination of price, processability and performance [1,2]. Recently, fluorinated polyimides have received considerable interest because of their optical transparency and improved solubility in organic solvents [3].

Fluorescence probe technology has received increasing interest for the investigation of polyimide films. In general, most of the polyimides are coloured, and show an extremely red-shifted intrinsic fluorescence [4,5]. This behaviour is not completely understood. The colour of these materials may be caused by the structure of the starting materials, the manufacturing process and intermolecular interactions between polyimide chains. The exceptions are polyimides made from hexafluoroisopropylidene-2,2'-bis(phthalic anhydride). These polymers are not coloured and show only slight fluorescence [3]. Several models have been discussed to explain

the fluorescence of polyimides. One of these involves the twisted intramolecular charge transfer (TICT) state [6,7]. The formation of a TICT state requires a perpendicular twist of the phenyl ring relative to the imide group. In this case, the electron is located in only one twisted subunit, and charge transfer can occur to the other subunit in the excited state. Another model for the emission mechanism in polyimides is based on charge transfer from the highest occupied molecular orbital (HOMO) to the lowest unoccupied molecular orbital (LUMO). This mechanism does not require twisting of parts of the molecule. Therefore it is called intramolecular charge transfer (ICT). The results obtained by CNDO/S3 calculations underline the possibility of this reaction pathway [8].

Polyimides have been used in many applications as thin films. Therefore fluorescence probe technology is a useful tool for the examination of the mobility and interactions in these materials. In general, two different methods can be used to study the polymer matrix. A fluorescence probe dissolved in the matrix provides information on the mobility in the polymer matrix [9,10]. On the other hand, a fluorescence probe covalently bonded at the polymer chain provides information on the mobility of the matrix itself [11,12]. For this reason, we synthesized probes containing the imide structure (to improve the solubility in the polyimide matrix) and a chromophore (which shows strong surroundings-dependent

* Corresponding author.

fluorescence). Stilbene molecules have been successfully applied as probes to investigate the molecular environments in different materials [13]. The stilbene structure is a reasonable probe because both fluorescence and isomerization are strongly influenced by the surrounding matrix [13]. Moreover, covalent bonding of stilbenes at an imide group in oligoimides leads to materials with covalently bonded chromophores [14]. Imide compounds with other chromophores were obtained by a similar procedure [15]. The materials prepared were obtained by the reaction between several dianhydrides and 3,7-diaminophenothiazinium chloride as well as thionine [15]. The properties of the materials obtained were very different from the starting materials, thionine and 3,7-diaminophenothiazinium chloride. Therefore we can conclude that the introduction of imide groups into several chromophores leads to a large change in the properties of the chromophores.

The goal of this work was to synthesize imide model compounds with covalently bonded stilbene groups for the photophysical investigation of polyimide films. These substances should have an improved solubility in polyimides and the stilbene group should act as a probe of the molecular environment. Other common fluorescence probes, such as triphenylmethane dyes [9] and several substituted dialkyl-aminostilbazolium salts [10,14], cannot be applied for probe experiments in polyimides because they can react with nucleophiles in the matrix (triphenylmethane dyes) or do not form transparent films because of their reduced solubility in the polymer matrix. The stilbene model compounds synthesized in this work are new compounds. They were studied in solution to determine their photophysical behaviour. Investigations in thin films were performed to provide more insight into their working principles as probes for applications in polymers. In addition, semiempirical quantum mechanical calculations were carried out to evaluate theoretically the experimental data and to provide more insight into the photochemistry of these new compounds.

2. Experimental details

2.1. Synthesis of the model compounds

The amounts of the starting materials for the synthesis of the imide model compounds are given in Table 1. Purified hexafluoroisopropylidene-2,2'-bis(phthalic anhydride) (Aldrich) was dissolved in 10 ml of anhydrous N-methylpyrrolidone at 80 °C. 2,5-Dimethoxy-4'-aminostilbene (Aldrich) was added together with 5 ml of anhydrous N-methylpyrrolidone. The mixture obtained was stirred at 80 °C for 11 h. This solution was slowly dropped into 150 ml of toluene and heated under reflux. The reaction water formed was continuously removed using a Dean–Stark apparatus. The toluene was removed in vacuum in a rotary still after the formation of the reaction water was complete. The residue obtained was added dropwise into 500 ml of ethanol. The precipitate was isolated and dried in vacuum. The diimide prepared from hexafluoroisopropylidene-2,2'-bis(phthalic anhydride) and 2,5-dimethoxy-4'-aminostilbene was obtained in 78% yield.

The imide model compounds prepared using the other anhydrides (pyromellitic dianhydride (Aldrich), 3,3',4,4'-benzophenone tetracarboxylic dianhydride (Aldrich) and phthalic anhydride) were synthesized in a similar manner. The yields of the imide model compounds obtained and their melting points are summarized in Table 1.

2.2. Film preparation

The polymeric material (0.05 g) (polymethylmethacrylate from Aldrich, a polyimide synthesized from hexafluoroisopropylidene-2,2'-bis(phthalic anhydride) (Aldrich) and 4,4'-diaminodiphenylmethane (Merck) in an equimolar ratio as described in Ref. [14]) was dissolved in 1 ml of propanone. A second solution (50 μl), consisting of propanone and the imide model compound, was added to the polymer solution. The solution obtained was coated onto a glass

Table 1
Summary of the imide model compounds synthesized (amounts of the starting materials 2,5-dimethoxy-4'-aminostilbene (DMAS) and anhydride, yields and melting points of the products)
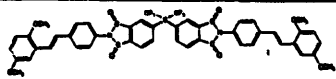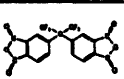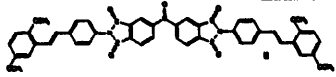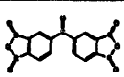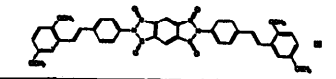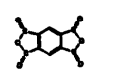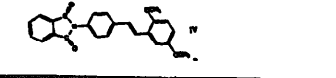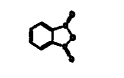
structure of the imide	anhydride structure	DMAS (mole)	anhydride (mole)	yield (%)	melting point (°C)
		0.018	0.009	78	266-268
		0.018	0.009	66	280-282
		0.018	0.009	58	365 (DSC)
		0.009	0.009	44	190-192

plate and dried at room temperature, first in a propanone atmosphere for 96 h and finally in air for 48 h. The absorbance of the film was about 0.4. The thickness of the film was between 6 and 7 μm.

2.3. UV absorption measurements

The UV absorption spectra of the imide compounds were recorded with a Cary 3 double-beam spectrophotometer in 1 cm cuvettes for solution experiments and as polymer films. Spectroscopic grade chloroform was obtained from Aldrich. Propanetriol triacetate (Aldrich) was purified by treating with potassium carbonate and drying with anhydrous magnesium sulphate, followed by fractional distillation in vacuum.

2.4. Stationary fluorescence measurements

The fluorescence spectra were measured using a Spex Fluorolog 212 spectrophotometer and an SLM-Aminco spectrometer. The slit width for emission was 2 mm corresponding to a spectral resolution of 5 nm. All fluorescence spectra were corrected by taking the sensitivity of the spectrometer into account. All solution spectra were measured using 1 cm quartz cuvettes. The emission was detected in perpendicular geometry. The films were recorded at an angle that resulted in a maximum fluorescence signal and a minimum scattering signal.

2.5. Time-resolved fluorescence measurements

Fluorescence lifetime measurements were performed at the Berlin storage ring for synchrotron radiation (BESSY) in the single bunch mode (repetition rate, 4.8 MHz) using single-photon counting detection. Using an excitation monochromator (focal length, 20 cm; Jobin Yvon), the excitation wavelength was selected from the spectral continuum of the synchrotron radiation. The pulses had a halfwidth of 500 ps (corresponding to the instrumental response of our system). Standard electronics from ORTEC were used for the time-correlated single-photon counting technique. The emission wavelength was selected using a similar monochromator (bandwidth, 20 nm). A microchannel plate photomultiplier (Hamamatsu R1564-U-01), cooled to -10 °C, was used for detection.

2.6. Irradiation experiments

The irradiation experiments were performed in 1 cm quartz cuvettes at room temperature. The equipment for the measurement of the quantum yields consisted of a high-pressure mercury lamp and a UV-visible spectrophotometer (Carl Zeiss Jena). Interference filters were applied to select the irradiation wavelength. The exposure of the samples was carried out perpendicular to the beam of the spectrophotometer. The difference between the incident quantum flux and

the flux behind the sample was measured and electronically integrated. The equipment was calibrated with a thermocouple. Further details on the working principles and accuracy of the equipment are given in Ref. [16]. For quantum yield calculations, the changes in absorbance were plotted as a function of the number of absorbed photons. The quantum yield was determined from the slope of the curve at a small number of absorbed photons. Further details were previously described [16]

2.7. Quantum mechanical calculations

AMPAC 5.0 from Semichem Inc. was used for all calculations. The AM1 method with the corresponding parameters was applied for energy minimizations. The gradients obtained after the calculations were used as a quality parameter.

3. Results and discussion

In a previous investigation, it was reported that substituted stilbenes possess high quantum yields of trans → cis photoisomerization [17]. In particular, stilbenes containing an amino group exhibit isomerization quantum yields of around 0.5 [17]. However, no information is available on the photoisomerization quantum yields of stilbenes containing an imide group covalently bonded at the aromatic skeleton. For this reason, model compounds were synthesized from 2,5-dimethoxy-4'-aminostilbene and different anhydrides as shown in Table 1. The reaction pathway for the synthetic procedure is given in Scheme 1.

Different anhydrides were used for the synthesis of the imide model compounds because of their different electronic influence (acceptor strength) on the photochemistry of the stilbene subunit. The compounds obtained are given in Scheme 2.

The UV absorption spectra obtained in propanetriol triacetate are given in Fig. 1. It can be seen that two bands exist in all the model compounds. They are located in the range 295–300 nm and at around 350 nm. The band at 295–300 nm is comparable with the absorption of substituted phenyl imides [18]. The absorption at around 350 nm is assigned to the stilbene skeleton ($\lambda_{max} = 353$ nm for 2,5-dimethoxy-4'-aminostilbene) (see Fig. 1). Only a slight influence of the imide skeleton is observed on the absorption at this wavelength.

The spectra obtained do not show an additional band, although two different chromophores are connected by covalent bonding forming a new conjugated system. This aspect is important in the consideration of the photoinduced isomerization of the double bond of the stilbene unit in the model compounds and the examination of the light stability. For this reason, irradiation experiments were carried out.

3.1. Irradiation experiments

For all irradiation experiments, monochromatic light was applied to excite the stilbene unit of the model compounds.

Reaction Mechanism
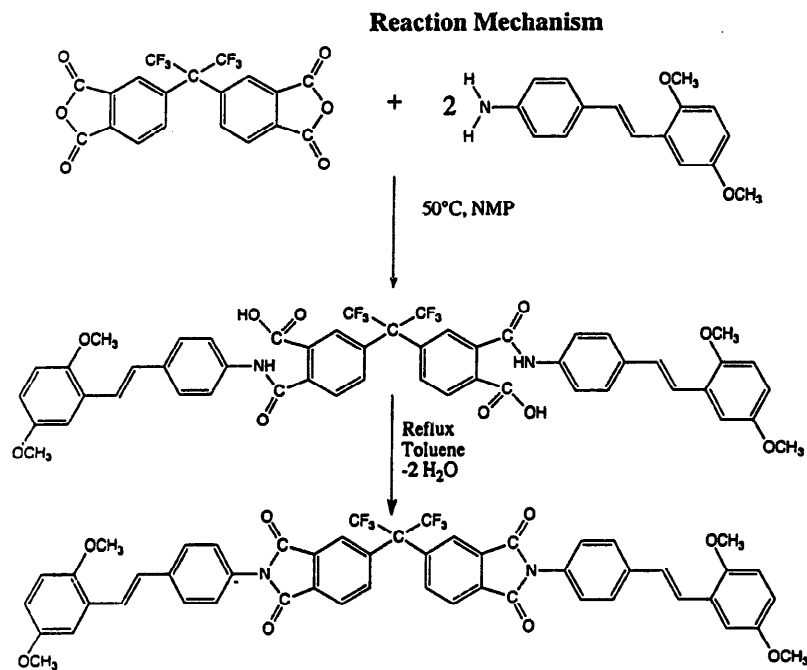
Scheme 1. Reaction scheme for the synthesis of stilbene-containing imide model compounds.
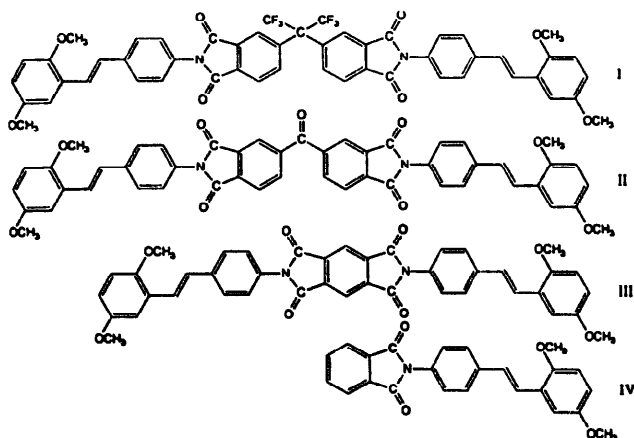
Scheme 2. Chemical structure of the model compounds consisting of stilbene covalently bonded at an aromatic imide.

Surprisingly, only small changes in the UV absorption spectra were found for all imide compounds used, and no isosbestic point was observed (see Fig. 2).

Additional irradiation experiments were carried out at 405 and 333 nm, after irradiation at 365 nm, to determine whether a photostationary composition exists after irradiation at 365 nm. The formation of a photostationary composition is dependent on the irradiation wavelength because the spectral contribution of each compound is different at each wavelength. No significant changes occur in the intensity of absorbance during irradiation at 405 and 333 nm after irradiation at 365 nm. Therefore the spectrum obtained at infinite irradiation time is equal to the spectrum of the photostationary composition. Furthermore, no information about the existence of a thermal activation barrier was found after exposure at 365 nm. All these results lead to the conclusion that photoisomerization is of minor importance for the imide com-

pounds investigated. The quantum yields for the decrease in absorbance determined at 365 nm are very small in comparison with the photoisomerization of 2,5-dimethoxy-4'-aminostilbene (see discussion below). They show no dependence on the nature of the solvent or the atmosphere (air, argon) as demonstrated in Table 2.

It is shown in Table 2 that 2,5-dimethoxy-4'-aminostilbene possesses a considerably higher quantum yield for the decrease in absorbance in comparison with the imide model compounds. The spectra obtained during irradiation indicate a high efficiency of trans–cis photoisomerization of 2,5-dimethoxy-4'-aminostilbene. An isosbestic point is observed at 299 nm. Similar high trans–cis photoisomerization efficiencies have also been reported for other substituted stilbenes [17].

The results indicate that the photochemistry of the imide model compounds is different from that of substituted aminostilbenes. Recently, a mechanism for the photolysis of substituted phenylimides on irradiation with polychromatic light from a medium-pressure mercury lamp has been proposed which describes the formation of different photolysis products, such as the corresponding anhydride and acid, a nonsubstituted imide (e.g. phthalimide) and nitrosobenzene. The cleavage of the (C=O)-N bond of the imide was reported to be the source of this reaction mechanism [19]. However, the formation of longer wavelength absorbing compounds, such as substituted nitrosobenzene, does not occur during photolysis with monochromatic light at 365 nm in our experiments (see Fig. 2). A higher energy is necessary for the cleavage of the (C=O)-N bond. Our results indicate that the stilbene skeleton is not able to sensitize the photolysis of the imide unit. The imide model compounds I-IV have sufficient photostability at an irradiation wavelength of 365 nm.
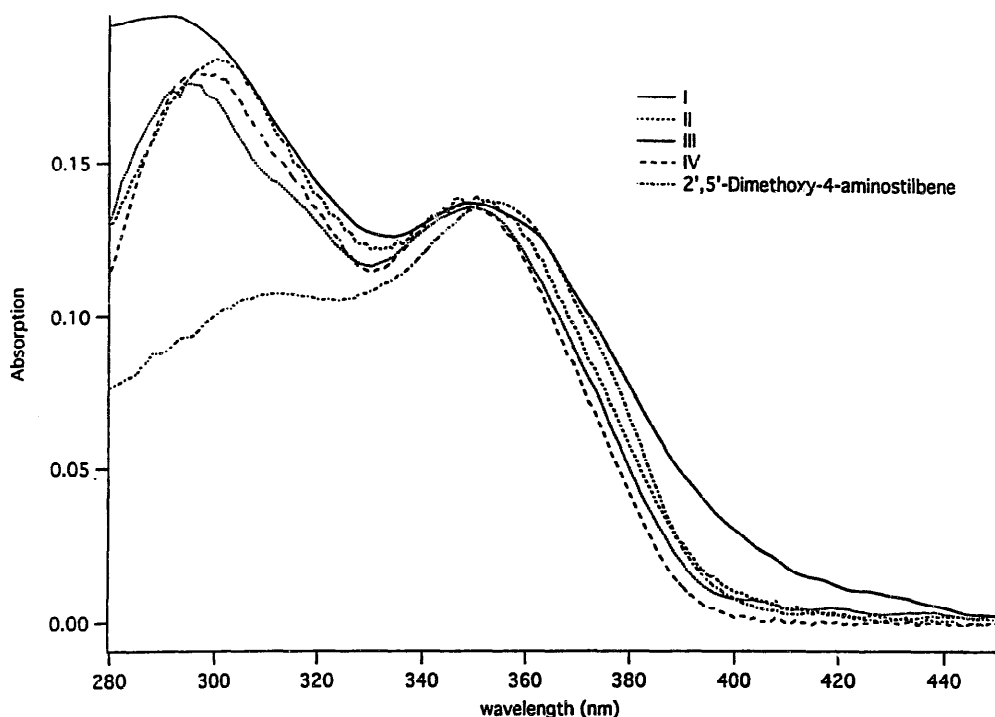
Fig. 1. UV absorption spectra for the model compounds I–IV and 2,5-dimethoxy-4'-aminostilbene in propanetriol triacetate at room temperature; spectra are normalized to the band with the highest wavelength.
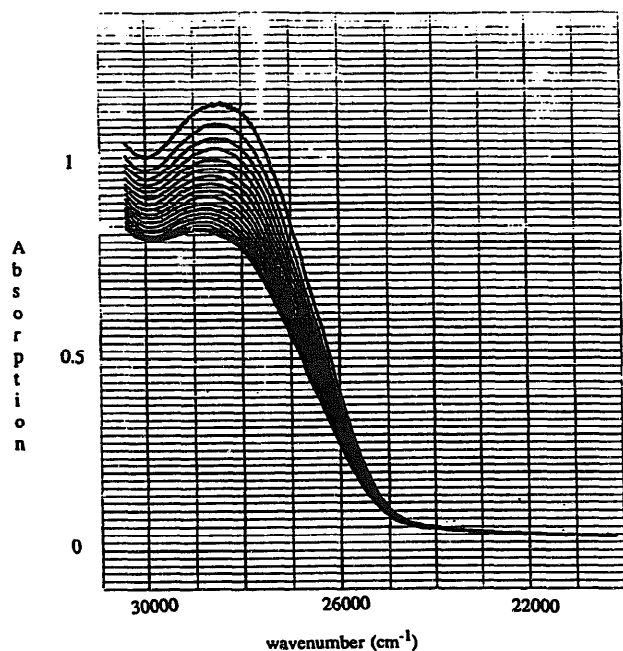

Fig. 2. Irradiation of model compound I in propanetriol triacetate (decrease in absorption) at room temperature using an irradiation wavelength of 365 nm.

3.2. Stationary fluorescence measurements

It is well known that substituted stilbenes show both efficient isomerization [17] and a matrix-dependent fluorescence [20]. The fluorescence experiments of the imide compounds were performed in a solution of propanetriol triacetate as well as in glassy polymers. These experiments are necessary to determine the emission behaviour of our stilbene

compounds which are covalently bonded at the imide group in different matrices.

The fluorescence spectra measured in propanetriol triacetate are shown in Fig. 3. As can be seen, only one fluorescence band with a maximum located at around 425 nm is observed for all the imide model compounds investigated. Dual fluorescence, as described for substituted aminostilbenes [20], does not occur in the solvent used. The fluorescence quantum yields are relatively low (less than 1%) for both 2,5-dimethoxy-4'-aminostilbene and the imide model compounds I–IV ($\Phi_f \approx 0.008$ for 2,5-dimethoxy-4'-aminostilbene). The fluorescence quantum yield of 2,5-dimethoxy-4'-aminostilbene is about twofold higher than that of imide compound III which has the highest value of all the imide compounds investigated in this work (see Fig. 3). As a result, we can conclude that chemical bonding of an imide structure at the stilbene skeleton leads to a decrease in the fluorescence quantum yield. All of these results indicate that non-radiative processes deactivate the excited state of the imide compounds I–IV, but the nature of these reactions is different from that described for the photochemistry of substituted stilbenes [17]. In addition, this non-radiative deactivation channel should depend on the matrix. For this reason, the fluorescence of I–IV was investigated in two different kinds of polymer.

The fluorescence spectra in polymethylmethacrylate (PMMA) films are comparable with those obtained in the viscous solvent propanetriol triacetate (Fig. 4). Furthermore, the unusual red-shifted fluorescence described for several imide compounds [4,5] was not found in our experiments. However, a different fluorescence behaviour of the imide compounds was found in a polyimide film (see Fig. 5). The

Table 2
Quantum yields for the reaction of the imide model compounds and 2,5-dimethoxy-4'-aminostilbene (reference) in different solvents

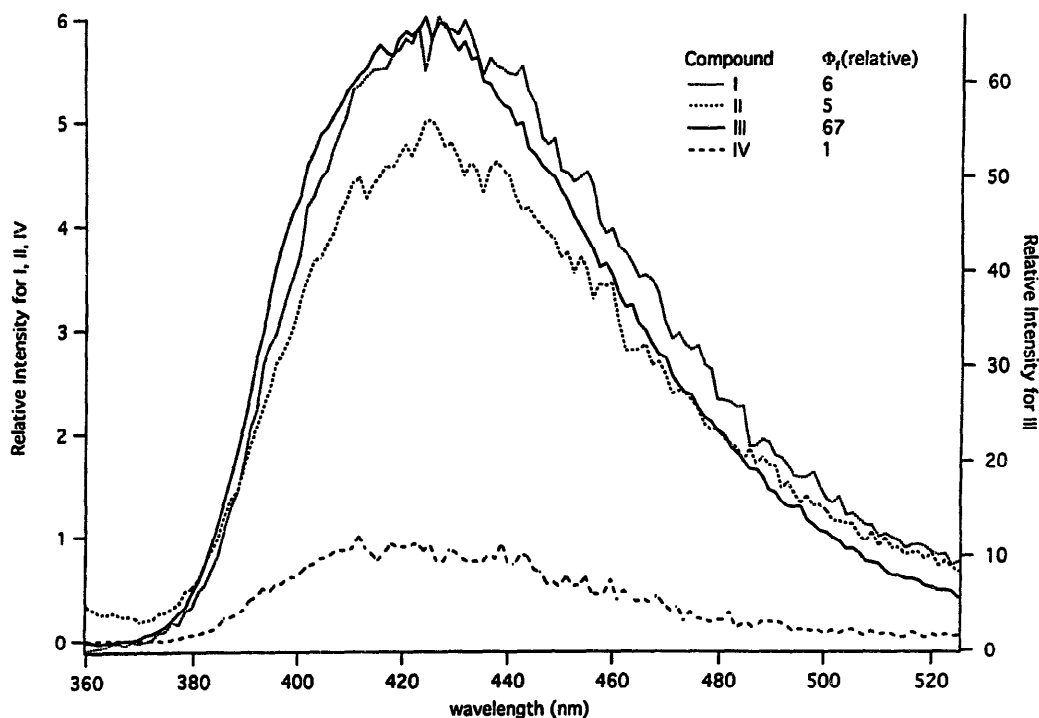| Compound	Propanetriol triacetate (air)	CHCl$_3$ (air)	CHCl$_3$ (argon)
I	0.0026	0.0012	0.0012
II	0.0017	0.0013	
III	0.0033	0.0034	
IV	0.0054	0.0015	
2,5-Dimethoxy-4'-aminostilbene	0.55	0.56	0.55

Fig. 3. Fluorescence spectra of the imide model compounds I-IV in propanetriol triacetate at room temperature; $\lambda_{exc} = 350$ nm.

polyimide was prepared containing 4,4'-diaminodiphenyl-methane and hexafluoroisopropylidene-2,2'-bis(phthalic anhydride).
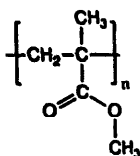
PMMA
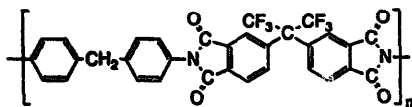
polyimide

Surprisingly, multiple fluorescence was found for the emission of I and IV in the polyimide matrix. One explanation for the occurrence of such a behaviour is the alignment of the polyimide chains. The alignment structure of the polyimide film can induce the formation of dimers which may exhibit a further radiative deactivation channel. This behaviour does not exist in amorphous polymers. Amorphous materials, e.g. PMMA, do not exhibit alignment of the polymer chains. A

schematic illustration of the imide model compound distribution in polymer matrices with and without alignment of the polymer chains is given in Scheme 3.

As can be seen, the imide model compound is statistically distributed in polymers without alignment. All changes in the emission behaviour are caused by the mobility of the polymer chains. An increase in the free volume in this matrix leads to an increase in the interactions between the probe and the polymer. On the other hand, a polymer with alignment can induce the formation of dimers or higher aggregates of the probe if the differences in the solubility between the polymer and the probe are small due to a similar structure.

3.3. Time-resolved fluorescence measurements

The results of stationary fluorescence measurements indicate the occurrence of a matrix-dependent fluorescence. Time-resolved experiments were carried out to obtain a better understanding of the photophysical processes influenced by the viscosity and temperature. Therefore time-resolved measurements were performed in propanetriol triacetate at different temperatures. This solvent becomes highly viscous with
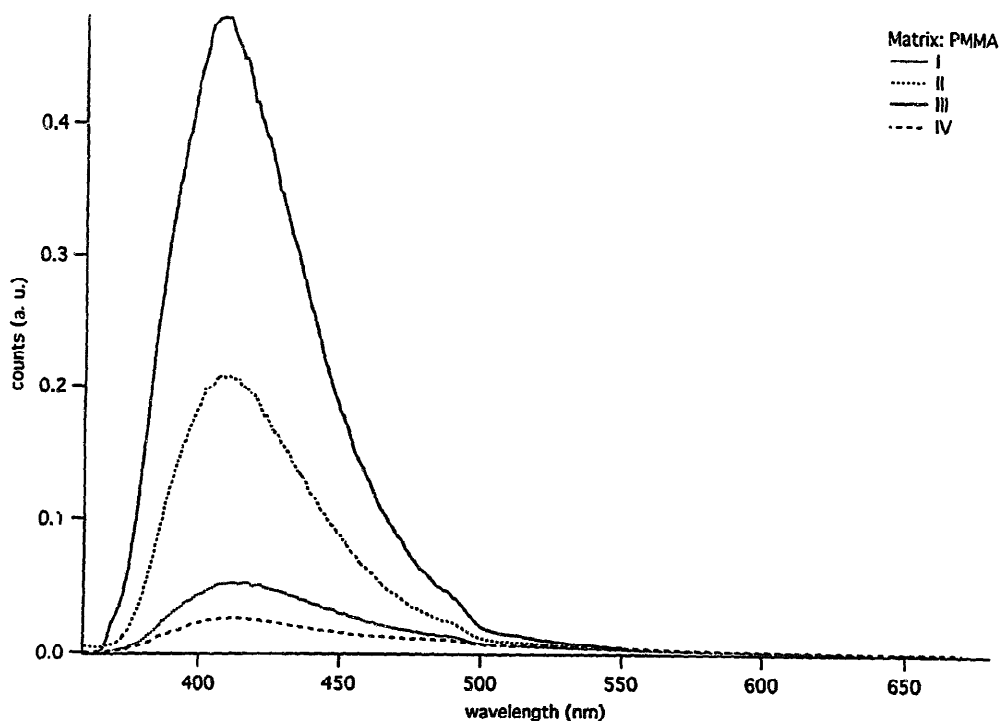
Fig. 4. Fluorescence spectra of the imide model compounds I–IV in polymethylmethacrylate at room temperature; $\lambda_{exc} = 350$ nm.
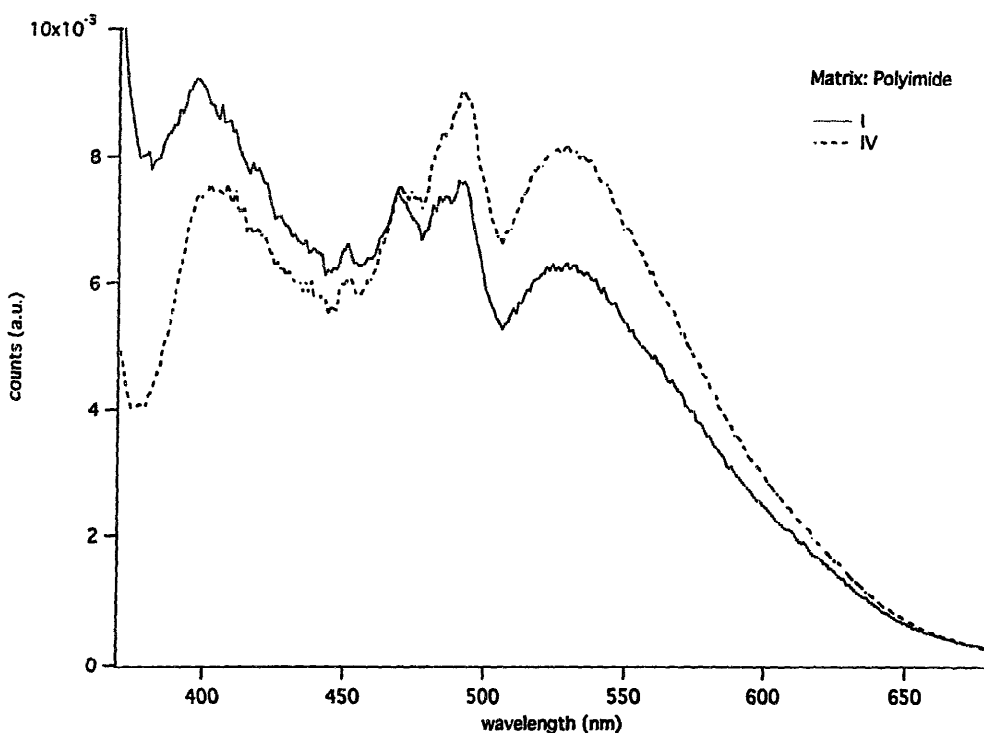
Fig. 5. Fluorescence spectra of the imide model compounds I and IV in a polyimide prepared from 4,4'-diaminodiphenylmethane and hexafluoroisopropylidene-2,2'-bis(phthalic anhydride) at room temperature; $\lambda_{exc} = 350$ nm.

decreasing temperature. In general, this technique is a reasonable basis for the examination of the fluorescence of compounds influenced by their surroundings. The decay curves obtained are multiexponential in all cases, but the course of the decay curves changes with decreasing temperature and increasing viscosity. A typical example of medium-dependent decay curves is given in Fig. 6. It was found in all measurements that the average fluorescence lifetime of the imide model compound increases with decreasing temperature of the surroundings in the liquid state of the solvent. A different behaviour of the lifetimes exists in the glassy state of the solvent.

The fluorescence decay curves indicate that a complex deactivation mechanism (multiexponential decay) occurs for
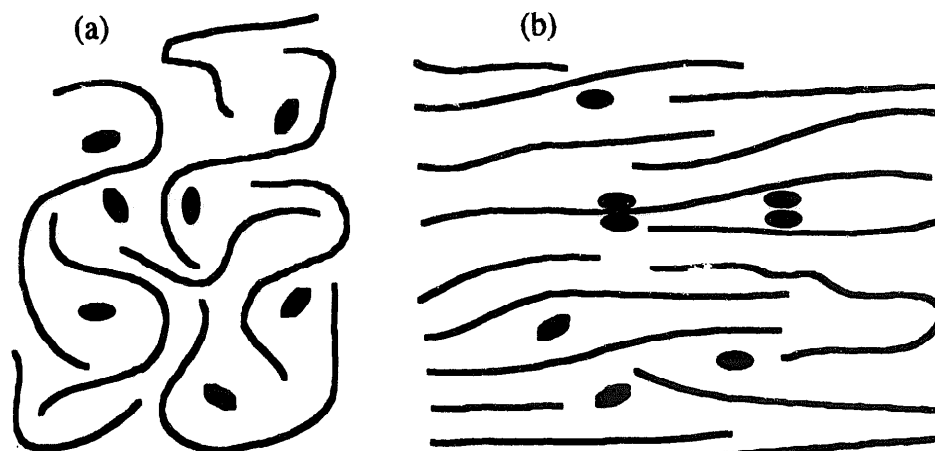
Scheme 3. Schematic illustration of the distribution of imide model compounds (elliptical symbols) in polymer matrices (bold lines): (a) polymer without alignment of the polymer chains; (b) polymer with alignment of the polymer chains.
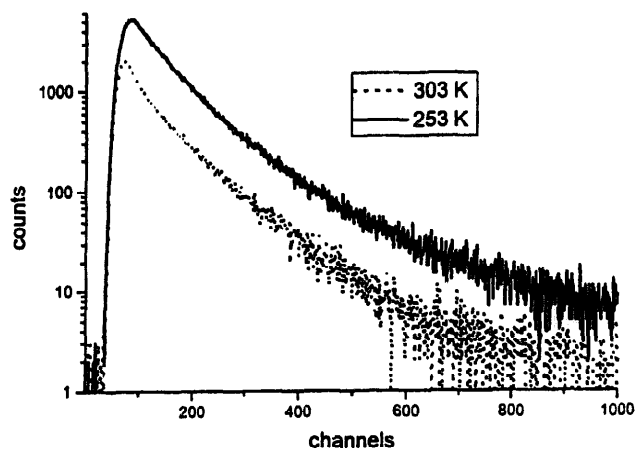

Fig. 6. Fluorescence decay curves of the imide model compound I in propanetriol triacetate at different temperatures; $\lambda_{exc} = 350$ nm; $\lambda_{em} = 400$ nm; slit width for emission and excitation, 2 mm (1 channel = 25 ps).

Table 3
Average fluorescence lifetimes (ns) (calculated according to Eq. (1)) of the imide model compounds I–IV in propanetriol triacetate at different temperatures

T (K)	I	II	III	IV
223	1.12	0.80	1.18	0.34
233		1.23	1.24	
243	1.41	1.22	1.53	0.89
253	1.17	0.93	1.36	1.56
263	0.84	0.57	1.40	0.58
273	0.85	0.46	1.16	0.44
283	0.88	0.25	1.18	0.55
303	0.43	0.27	0.74	

the imide model compounds I–IV. For a preliminary discussion of these results, the average fluorescence lifetime was calculated using Eq. (1)

$$\langle \tau_f \rangle = \frac{\sum_i^n \alpha_i \tau_i}{\sum_i^n \alpha_i} \approx \frac{1}{\Sigma k_f + \Sigma k_{nr}} \tag{1}$$

where $\langle \tau_f \rangle$ is the average fluorescence lifetime, α_i is the pre-exponential factor, τ_i is the fluorescence lifetime, n is the number of fluorescence lifetimes, k_f is the rate constant for the radiative process and k_{nr} is the rate constant for the non-radiative process.

The average lifetimes obtained are summarized in Table 3. As can be seen, the $\langle \tau_f \rangle$ values begin to increase with decreasing temperature and increasing viscosity. The reduced mobility in the system, induced by the decrease in temperature, leads to a decrease in the rate constant of the non-radiative processes causing an increase in the $\langle \tau_f \rangle$ values. Furthermore, a decrease in the $\langle \tau_f \rangle$ data is observed at very low temperatures, comparable with the glassy state of the solvent. We

believe that additional fast processes can be measured by our time-resolved equipment in the glassy state of the solvent because these processes occur with a lower efficiency in such a matrix. On the other hand, measurements of these reactions at elevated temperatures (liquid state) are limited due to the given time resolution. The following aspects can be discussed to explain the complex fluorescence behaviour of our compounds.

1. A simplified two-state reaction model can be assumed to determine the photophysical properties in the excited state. It can be described by a consecutive reaction in the excited state ($A^* \rightarrow B^*$). The excited state of A (A^*) can fluoresce while the radiationless deactivation of B^* occurs to the ground state. The compound B relaxes rapidly to the geometrically more stable conformation A. The efficiency of this reaction is dependent on both the temperature and viscosity of the surroundings.

2. Different geometrical conformations exist for A. However, an optimal geometrical structure is responsible for the formation of B in the excited state. The fluorescence decay curve measured indicates an ensemble of all geometrical conformations of A^* which have different rate constants for the reaction $A^* \rightarrow B^*$. As a result, the fluorescence decay behaviour can be described by a distribu-

tion of different conformers which contribute differently to the emission.

3. The relaxation of the solvent dipoles influences the emission behaviour of the model compounds I–IV. Models of solvent dynamics and charge transfer [21,22] can be applied for the discussion of the decay curves.

Charge transfer can occur in our model compounds from a thermodynamic point of view. Eq. (2) can be taken into account for the consideration of this reaction [22]

$$\Delta G_{ET} = E_D^0 - E_A^0 - E_{00} - E_C \qquad (2)$$

where ΔG_{ET} is the free reaction enthalpy for electron transfer, E_D^0 is the half reaction redox potential for oxidation, E_A^0 is the half reaction redox potential for reduction, E_{00} is the excitation energy and E_C is the Coulomb energy.

Therefore the molecule was cut into two parts: the phthalimide and stilbene subunits. Electron transfer occurs from the donor (D) to the acceptor (A). We assume that the stilbene acts as the donor and the phthalimide acts as the acceptor. Our quantum chemical results show the validity of this assumption. For the calculation of the free reaction enthalpy for electron transfer, we substitute the corresponding values for the phthalimide and stilbene into Eq. (2) ($E_A^0 = -0.41$ V for the phthalimide [23]; $E_D^0 \approx 1.95$ V (this value was obtained by a correlation of the HOMO energy (AM1 hamiltonian) vs. the E_D^0 values within a series of selected hydrocarbons [24]); $E_{00} \approx 3.51$ eV (value from the absorption maximum of compound IV; all polarographic data were corrected vs. a normal hydrogen electrode (NHE))). Thus we obtain a value for ΔG_{ET} of about -1.15 eV (approximately 111 kJ mol^{-1}). This value shows that photoinduced charge transfer, e.g. in the model compound IV, has a high exothermic value. The Coulomb energy was neglected in these considerations because the solvent propanetriol triacetate has a high polarity. Polar solvents show little contribution to the free enthalpy for electron transfer [22]. Furthermore, the electron affinity of the imide also influences the efficiency of the charge transfer reaction. Similar investigations on several phenyl imides support this idea [25]. The biradicaloid structure formed possesses a high dipole moment. The energy of such molecules can decrease in polar solvents due to the stabilization of the polar surroundings. Thus a stabilized excited state is reached after charge transfer and solvation. It deactivates mainly by a radiationless process because of the small energy difference between the excited state and the ground state. This behaviour in the excited state can explain the dominance of non-radiative processes at room temperature. A decrease in temperature leads to a decrease in the rate constant of assumed electron transfer. Thus an increase in the fluorescence efficiency can be observed in the solvent. The increase in the average fluorescence lifetime in the liquid state underlines this result (see Table 3).

All the results together lead to the conclusion that a complicated photophysical behaviour exists for the imide model compounds I–IV. Photoinduced charge transfer seems to control the behaviour of the molecule in the excited state.

Other typical photoreactions, such as photoinduced isomerization of the double bond, are of only minor importance. For this reason, quantum mechanical calculations were carried out to examine our molecules from a theoretical point of view. They are a useful tool for studying the electronic structure of possible reaction products after excitation of selected imide model compounds. They also give the opportunity to calculate possible electronic transitions in the UV absorption spectrum.

3.4. Quantum mechanical calculations

The imide model compounds I–III have a relatively high molecular weight. For this reason, we applied semiempirical calculations on the basis of AM1 to optimize the geometry and to calculate the spectroscopic transitions from the ground state to the excited state, although this treatment was accompanied by several simplifications. All calculations were carried out without the methoxy groups bonded at the stilbene unit of molecules II–IV (calculations for compound I did not lead to reasonable results because of convergence problems). Additional calculations were carried out for model compound IV containing methoxy groups. The results obtained show that the geometry (dihedral angles, bond angles, bond lengths) for both imide molecules does not exhibit significant changes in the presence or absence of methoxy groups at the stilbene unit. Therefore it is reasonable to remove the methoxy groups of model compounds II–IV for the calculation because the molecule should be as simple as possible for theoretical considerations.

The first step in the theoretical investigation of the photophysical behaviour was the calculation of the molecular orbitals for compounds II–IV (without methoxy groups). The results are shown in Fig. 7. Surprisingly, it was found that charge transfer occurs from the stilbene skeleton to the imide group for all compounds calculated. This theoretical result stands in accordance with our experimental results, and underlines the occurrence of charge transfer from the HOMO to the LUMO. The localization of the atomic orbital coefficients occurs on only one subunit at the HOMO and LUMO. The atomic orbitals in the other part of the molecule are close to zero. Furthermore, the structures of the frontier orbitals show that the stilbene has a donor function because the electron is localized at this subunit in the HOMO. On the other hand, the LUMO shows the acceptor function of the phthalimide group. The structures of both of these frontier orbitals are different from those described for common stilbenes [13]. The charge transfer which occurs from the HOMO to the LUMO is one possible way to describe the behaviour of our compounds.

The different spectroscopic transitions were calculated to obtain information about the contribution of each configuration to the Franck–Condon state. The results are summarized in Table 4. The HOMO–LUMO configuration can be found in higher excited states, whereas S_1 is represented by a mainly locally excited state of the stilbene subunit. The oscillator

Table 4
Quantum mechanical results for the calculation of the Franck–Condon states (singlets) for the imide model compounds II–IV

Imide compound	State	Energy (eV)	Oscillator strength	MO configuration (singlet excitation)	Contribution (%)
IV	S_1	3.73	1.1618	HOMO→LUMO+1	52
				HOMO→LUMO+2	38
	S_2	4.34	0.0100	HOMO→LUMO	82
	S_3	4.86	0.0016	HOMO→LUMO+3	46
	S_4	5.11	0.0024	HOMO→LUMO+3	18
				HOMO−1→LUMO+1	40
				HOMO−1→LUMO+2	20
III	S_1	3.80	0.0300	HOMO→LUMO	72
	S_2	3.85	0.0000	HOMO−1→LUMO	72
	S_3	3.88	2.2570	HOMO→LUMO+2	48
				HOMO→LUMO+3	42
	S_4	3.92	0.0477	HOMO→LUMO+2	48
				HOMO→LUMO+3	44
II	S_1	4.24	1.0467	HOMO→LUMO+4	96
	S_2	4.29	0.7889	HOMO→LUMO+5	96
	S_3	4.79	0.0089	HOMO→LUMO	54
				HOMO→LUMO+1	44
	S_4	4.80	0.0170	HOMO−1→LUMO	68
				HOMO−1→LUMO+1	30
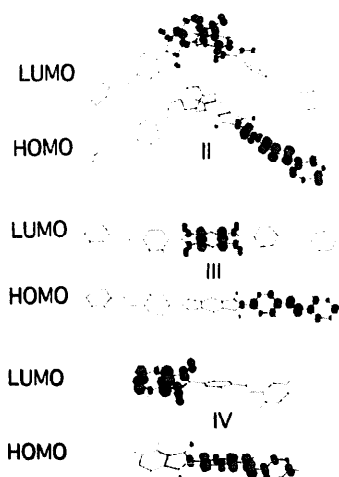
Fig. 7. Selected molecular orbitals for the compounds II–IV calculated with the AM1 hamiltonian.

Table 5
Singlet energies and dipole moments for some relaxed excited states (optimized geometry) of the imide model compounds calculated by AM1

Imide compound	State	Energy (eV)	Dipole moment (D)
IV	S_1	3.27	3.69
	S_2	3.29	4.49
	S_3	3.52	25.3
III	S_1	2.50	26.1

strength is small for the excited state in which the HOMO–LUMO configuration ($\pi_z \rightarrow \pi_y$ transition) dominates, but is large for all locally excited states. All these quantum mechanical results indicate that the introduction of an imide group at the stilbene skeleton leads to a change in the electronic properties of the stilbene molecule. The charge transfer from the HOMO to the LUMO can be considered as an additional reaction pathway that dominates in the case of these imide model compounds. Such molecules possess a full separated charge in one unit of the molecule (stilbene or phthalimide) which can be sufficiently stabilized by the polar surroundings (decrease in the energy for the excited state). Large dipole moments, induced by charge transfer in the molecule, may be a source of non-radiative processes because of strong inter-

actions with the polar environment. Thus the additional stabilization of charge transfer by a polar solvent yields an energy for this excited state which is not very different from that of the ground state. As a result, the deactivation of the solvated charge transfer to the ground state occurs by a mainly radiationless process.

The influence of charge transfer becomes clearer if we consider the excited state with full relaxed geometry. The results are summarized in Table 5. The energy of this state is smaller than that of the related Franck–Condon state. Furthermore, the relaxed excited state possesses a considerably higher dipole moment. This result underlines the occurrence of charge transfer in these compounds. This effect is strongly reflected in compound III. The Franck–Condon state has a very small dipole moment due to the high symmetry of this molecule. On the other hand, the relaxed excited state possesses a dipole moment which is considerably larger. Molecules having a high dipole moment can be stabilized by polar solvents. Polar solvents lead to a further decrease in the energy of the excited state. The resulting energy of such an excited state has a small gap to the ground state.

Another observation during our quantum mechanical calculations was the change in geometry during the transition from the Franck–Condon state to the corresponding relaxed excited state. For example, the phenyl rings of the stilbene skeleton are pre-twisted at around 17° in the Franck–Condon state. However, in the corresponding relaxed excited state, this stilbene subunit becomes planar. Furthermore, the change in the dihedral angle of the phenyl ring in the stilbene unit is accompanied by a change in the bond lengths of both the olefinic double bond and the adjacent single bonds. These changes can be called vibrational modes which are necessary to explain the photochemistry and charge transfer of our compounds.

In this work, the TICT model [6] was not applied to describe the charge transfer of our imide model compounds, although an explanation using this model may be possible. The ICT occurring in the imide model compounds is sufficient to explain some of their photophysical properties.

4. Conclusions

In this paper, we have discussed the photophysical properties of stilbenes with chemically bonded imide groups. The model compounds I–IV are new compounds. They were synthesized from the same stilbene amine and different anhydrides. The introduction of imide structures into the stilbene skeleton results in a change in the typical properties of stilbene. Certain photoreactions, such as photoisomerization, have minor importance in the photochemistry of these substituted stilbenes, whereas other photoreactions, e.g. intramolecular charge transfer, seem to control their photochemistry. As a result, model compounds I–IV possess sufficient light stability, but also show a low efficiency for fluorescence. The large dipole moments of the intramolecular charge transfer state, calculated by the AM1 method, can explain the phenomenon of fast non-radiative processes. Polar solvents lead to an additional stabilization of the excited states with charge transfer properties. Thus the energy difference between the fully relaxed solvated molecule in the excited state and the ground state becomes extremely small, and the deactivation of the excited state occurs by a mainly radiationless process. This photochemical behaviour may be of interest for several photonic applications. Furthermore, the imide model compounds I–IV may be applied as fluorescence probes for the characterization of polymeric materials, because they show a surroundings-dependent fluorescence, although the alignment of the matrix needs to be considered for a complete discussion. Finally, an examination of model compounds I–IV using other photophysical methods, such as transient absorption, may provide additional information for a better understanding of the photophysical behaviour in the excited state.

References

[1] D. Wilson, H.D. Stenzenberger, P.M. Hergenrother (Eds.), Polyimides, Chapman and Hall, New York, 1990.
[2] K.L. Mittal, Polyimides, Synthesis, Characterization and Application, vol. 1, Plenum, New York, 1984.
[3] A.K.St. Clair, T.L.St. Clair, W.S. Slemp, in: W.D. Weber, M.R. Gupta (Eds.), Recent Advances in Polyimide Science and Technology, Proceedings of the Second International Conference on Polyimides, Mid-Hudson Section, Society of Plastics Engineers, 1987, pp. 16–36.
[4] J.M. Salley, C.W. Frank, Polymer Preprints 33 (1) (1992) 878–879.
[5] K. Horie, Photophysics, photochemistry, and photo-optical effects in polymer solids, in: H. Ito, S. Tagawa, K. Horie (Eds.), Polymeric Materials for Microelectronic Applications in Science and Technology, ACS Symposium Series 579, American Chemical Society, Washington DC, 1994, pp. 2–12.
[6] W. Rettig, Angew. Chem., Int. Ed. Engl. 25 (1986) 971–988.
[7] E. Wachsmann, P.S. Martin, C.W. Frank, Cure studies of PMDA-ODA- and BTDA-ODA-based polyimides by fluorescence spectroscopy, in: J.H. Lupinski, R.S. Moore (Eds.), Polymeric Materials for Electronics Packaging and Interconnection, ACS Symposium Series 407, American Chemical Society, Washington DC, 1989, pp. 26–48.
[8] G. Arjavalingam, G. Hougham, J.P. LaFemina, Polymer 31 (1990) 840–844.
[9] B. Strehmel, V. Strehmel, H.-J. Timpe, K. Urban, Eur. Polym. J. 28 (1992) 525–533.
[10] B. Strehmel, V. Strehmel, M. Younes, S. Wartewig, Prog. Coll. Polymer Sci. 90 (1992) 83–87.
[11] B. Strehmel, C.W. Frank, Polymer Preprints 36 (1) (1995) 385–386.
[12] B. Strehmel, C.W. Frank, W. Abraham, M. Garrison, Modified polydimethylsiloxanes with fluorescent properties, in: N. Auner, J. Weiss (Eds.), Organo-Silicon Chemistry III, VCH, Weinheim, in press.
[13] H. Meier, Angew. Chem. 104 (1992) 1425–1446.
[14] V. Strehmel, C.W. Frank, Polymer Preprints, 36 (1) (1995) 477–478.
[15] H.M. Gajiwala, R. Zand, Macromolecules 26 (1993) 5976–5983.
[16] H. Baumann, K. Behrmann, H. Jahnke, W. Ortmann, G. Waldmann, Automatic spectrophotometric determination of quantum yields with an electronic actinometer, J. Signalaufzeichnungsmater. 11 (1983) 385–394; Chem. Abstr. 100 (1984) 77083v.
[17] D.H. Waldeck, Chem. Rev. 91 (1991) 415–436.
[18] C.E. Hoyle, D.T. Anzures, J. Polym. Sci., Polym. Chem. 30 (1992) 1233–1245.
[19] C.E. Hoyle, D. Creed, R. Nagarajan, P. Subramanian, E.T. Anzures, Polymer 33 (1992) 3162–3168.

[20] J.F. Letard, R. Lapouyade, W. Rettig, J. Am. Chem. Soc. 115 (1993) 2441–2447.

[21] K. Yoshihara, K. Tominaga, Y. Nagasawa, Bull. Chem. Soc. Jpn. 68 (1995) 696–712.

[22] G.J. Kavarnos, Fundamentals of Photoinduced Electron Transfer, VCH, New York, Weinheim, Cambridge, 1993.

[23] K. Schwabe, Polarographie und Konstitution organischer Verbindungen, Akademie-Verlag GmbH, Berlin, 1957.

[24] H.G.O. Becker, Einführung in die Photochemie, Verlag der Wissenschaften, Berlin, 1983.

[25] M. Hasegawa, I. Mita, M. Kochi, R. Yokota, J. Appl. Polym. Sci.: Part C: Polym. Lett. 27 (1989) 263–269.